Long-term Monitoring of Salt Movement in Masonry Materials

FRICK, JÜRGEN[1]; GABRIELLI; ELENA[2]; COLLA, CAMILLA[3];GRÜNER; FRIEDRICH[4]

ABSTRACT: The recrystallization of salts due to changes in moisture content is one of the major damage functions in historic materials like natural stones, tiles, plasters, and mortars. This paper presents results of a long-term wireless monitoring of salt and moisture movement at a test wall. Within the EU-project "Smart monitoring of Historic Structures – SMooHS (www.smoohs.eu), a potential difference measurement node was developed in combination with ion-selective electrodes based on silver/silver-chloride for the detection of chloride salts in porous masonry materials. Masonry walls placed in outdoors climate conditions in Bologna were preloaded by capillary suction with diluted NaCl solutions for several months. The salt migration and content were monitored with the developed wireless sensor system over a period of more than three years. Different regimes of potential difference signals were identified dependent on sensor position, moisture content and climate conditions. A comparison with a model for hygrothermal analysis shows comparable results.

Keywords: Masonry, wireless sensor, ion-selective electrodes, capillary suction, deterioration, salt decay.

NOTATION

ISE ion-selective-electrode;

1 INTRODUCTION

Within the EU-project "Smart monitoring of Historic Structures – SMooHS [1] several advanced monitoring devices were developed integrated in a network of wireless sensing nodes. One of them was an electrometer to measure potential differences. By the use of ion-selective electrodes (ISE) information about the movement of salts in porous materials could be gathered. In 2010 model masonry walls were built in Bologna and subjected to outdoor climate conditions. To simulate a capillary suction the walls were subjected to the uptake of brine solutions from a basin at the wall base. One of these walls was equipped with ISEs in horizontal and vertical profiles to monitor the movement of salts within the wall by the use of potential difference measurements. First results show qualitatively comparable results according to salt analyses taken after eight month of exposure and seasonal changes were analysed [2, 3]. The setup of the wall together with additional laboratory experiments was used by other authors to calculate moisture and salt movement with a novel coupled multiphase model for hygrothermal analysis of masonry structures, which allows predicting stress induced by salt crystallization [4, 5]. The present paper compares results of the hygrothermal model calculations with a detailed analysis of several seasonal periods within the first year of exposure.

[1)] Dr., Materials Testing Institute (MPA) University of Stuttgart, Department NDT, juergen.frick@mpa.uni-stuttgart.de
[2] DICAM University of Bologna, elena.gabrielli4@unibo.it
[3)] Dr., DICAM University of Bologna, camilla.colla@unibo.it
[4] Dr., Materials Testing Institute (MPA) University of Stuttgart, Department Protection of Buildings and Plants, friedrich.gruener@mpa.uni-stuttgart.de

2 EXPERIMENTAL

2.1. Test wall

The experiments were performed at a 2-header masonry wall made of solid brick units (25 x 12 x 5.5 cm^3) and nominal 1 cm thick hydraulic lime mortar joints. Red bricks and natural hydraulic lime mortar are typical historic masonry construction materials. Several natural stone inclusions have been inserted in the wall front side, at 3 different heights, at masonry course 6, 10, and 16 (Figure 1).

After curing inside, the wall has been moved outdoors and exposed to ageing in natural climatic conditions. Subsequently to electrodes installation in June 2010, brine solution capillary rise from the wall base was simulated by a sodium chloride solution at low concentration (0.05 mass-%, which corresponds to 0.0086 mol/l). The brine solution at the wall base had a height of around 3.5 cm. It was kept as constant as possible within two periods, from 21st July 2010 to 6th December 2010 and from April 2011 to November 2011. Sodium chloride was used as test solution, because of the sensitivity of the ISEs to chloride.

The migration of brine in the wall was studied using two self-developed wireless monitoring systems: a potential difference measuring device (8 channels, input resistance 100 GΩ) and a device for the measurement of environmental parameters (combined temperature and relative humidity of air (SHT15, Sensirion AG), and internal wall temperature (PT100, course 3 (2 and 10 cm depth) and course 9 (6 cm depth) on the front (Figure 1) and course 2 (10 cm depth) on the rear side)).

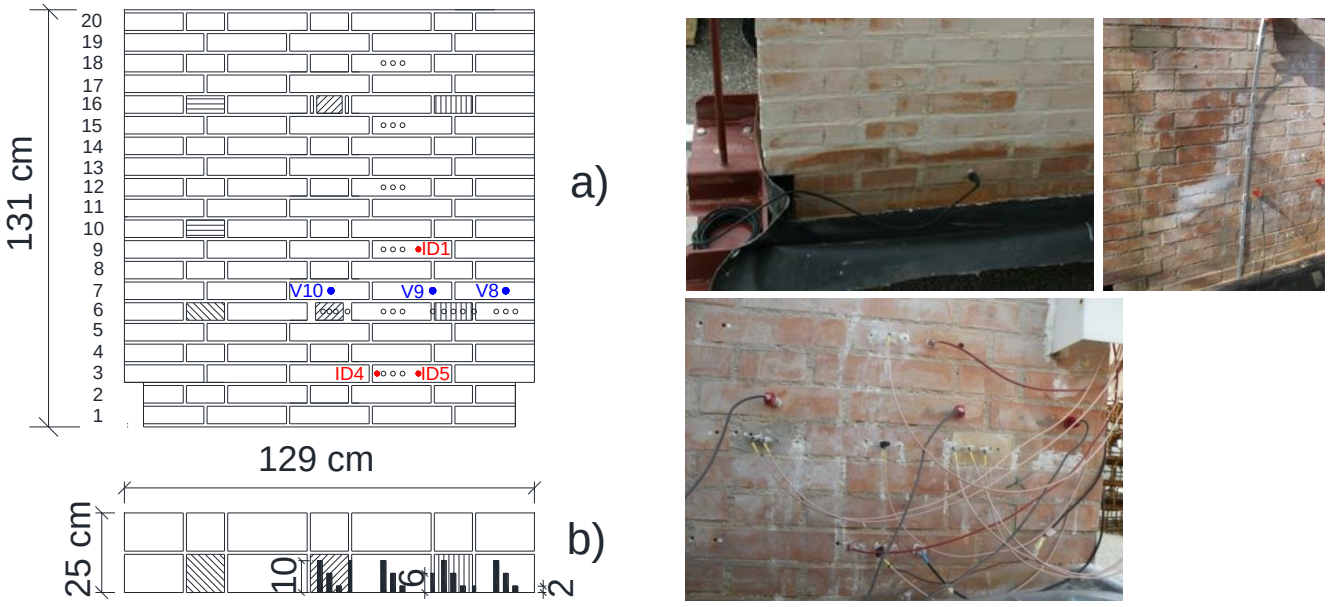

Figure 1. Left: Brick masonry wall, distribution of potential (in black) and temperature sensors (in red): a) front view, b) horizontal section at course 6. Right top: Reference electrode on the rear side (at installation) and salt efflorescence at the front side (after 8 months). Right bottom: Detail of vertical and horizontal profile at the front side (3rd May 2011).

The ISE have been distributed on the wall following both a horizontal semi-profile on the 6th masonry course from the base (this corresponds to a sensor height of 36 cm above the wall base), and a vertical profile along a section at 18 cm from the wall centreline, at 6 heights, from course 3 to 18 (that is from about 16.5 cm to 114 cm above the wall base). ISEs were inserted in 3 different depths (2 cm, 6, cm and 10 cm) in the different masonry components of the wall: bricks, mortar joints and two different natural stones by the use of a mortar consisting of LUDOX® HSA Colloidal Silica (Grace Davison) as binder and KSE Filler A and B (Remmers Baustofftechnik GmbH) as filling materials. The reference electrode (row 2, depth 10 cm on the rear side) fitted tight in a borehole without mortar. To guarantee a good contact to the pore solution Silica gel powder was put in front of the reference

electrode tip. In general reference electrode and measurement device could be re-used, only the ISEs should be replaced for new measurements.

2.2. Potential difference measurements

The ISE consist of a silver wire (99.99 % pure silver) with an electrochemically deposited silver chloride coating and a final drop of molten silver chloride on it. The measured potential difference is the potential between the ion selective electrode and a saturated reference electrode. A saturated silver/silver chloride electrode (Schott Instruments 9801/85) was used as reference.

The measured potential difference E_M follows Nernst law and can be written [6]:

$$E_M = E_{Ag/AgCl} - E_{\mathrm{Ref}} = E^0_{Ag/AgCl} - \frac{RT}{F} \ln a_{Cl^-} - E_{\mathrm{Ref}} \qquad (1)$$

$$\text{with } a_{Cl^-} = \gamma_{\pm}\, c_{Cl^-}$$

Here, $E_{Ag/AgCl}$ is the potential of the ISE, R is the gas constant, F the Faraday constant, T the absolute temperature in K, a_{Cl^-} the chloride activity, E_{Ref} has the same form as $E_{Ag/AgCl}$ in case of a saturated silver/silver chloride reference electrode, $\gamma_{\pm}$ the mean activity coefficients, and c_{Cl^-} the chloride concentration. $E^0_{Ag/AgCl}$ is the standard potential of the silver/silver chloride equilibrium reaction.

Calibration measurements were performed in different solutions with varying chloride content. The results are shown in Figure 2. The concentration dependence follows Nernst law and is in good accordance with the theoretical values. Small differences could be due to junction potentials at the reference electrode [6]. Mean activity coefficients $\gamma_{\pm}$ for NaCl and $CaCl_2$ solutions were taken from [7, 8].

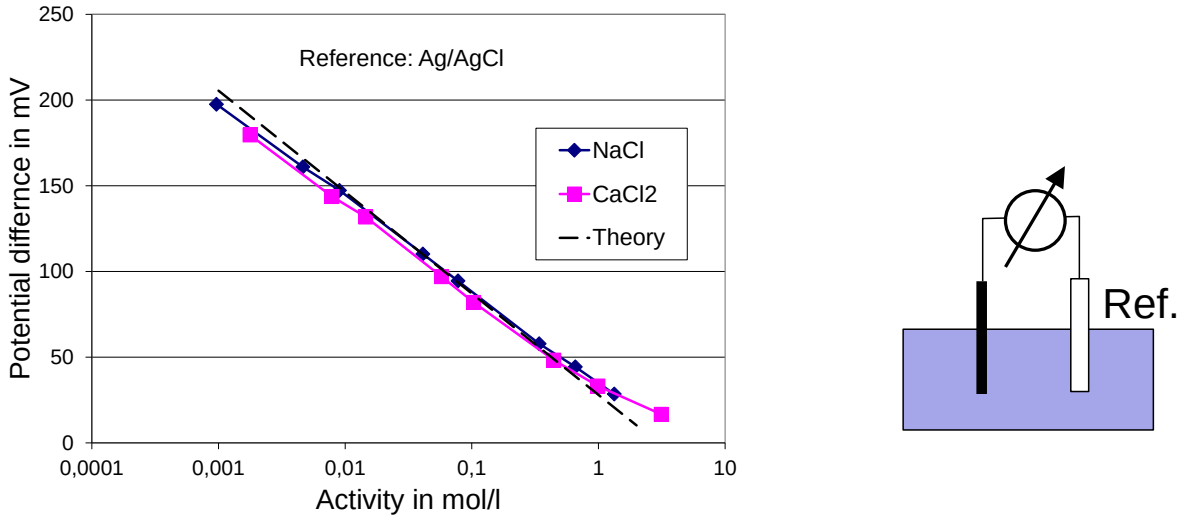

Figure 2. Left: Potential difference within different solutions. Reference: saturated Ag/AgCl. Right: Measurement principle.

If the temperature between the Ag/AgCl ISE and the reference electrode (saturated Ag/AgCl) is equal, the term $E^0_{Ag/AgCl}$ is eliminated in (1) and the measured potential E_M is given by [9]:

$$E_M = \frac{RT}{F}\left(ln\, a^{Ref}_{Cl^-} - ln\, a_{Cl^-}\right) \qquad (2)$$

This can be transformed to estimate chloride activity:

$$\ln a_{Cl^-} = \ln a_{Cl^-}^{Ref} - \frac{FE_M}{RT} \quad (3)$$

If potential difference and temperature are measured and the chloride activity of the reference electrode is known the chloride activity of the solution can be calculated. The reference electrode has a concentration of 3 mol/l KCl [10] and a mean activity coefficient $\gamma_{\pm}$ = 0.714 [7].

2.3. Drill dust samples

After the first period of capillary suction with brine solution (around 4 months from 21st July to 6th December 2010) the wall was exposed without additional brine solution to outdoor conditions until end of March 2011. On 29th and 31st March 2011 drill dust samples of masonry component materials have been sampled from the test wall in order to determine, by laboratory analysis, the distribution of salt content in the masonry [2, 3]. Dust samples within a vertical profile were analysed in depth steps of 1 cm by ion chromatography. The results are shown in Table 1.

Table 1. Concentrations of anions and cations (only 0 – 1 cm) in mass-% in bricks within the vertical profile. Chloride concentrations in bold. The conductivity in µS/cm of the eluates is given.

Row	Depth	F^-	Cl^-	NO_3^-	SO_4^{2-}	Cond.	Sum anions
3	0 – 1 cm	0.010	**0.011**	0.004	0.062	113	0.087
	1 – 2 cm	0.012	**0.004**	0.001	0.104	194	0.121
	2 – 3 cm	0.005	**0.004**	0.002	0.035	197	0.046
	3 – 4 cm	0.009	**0.006**	0.001	0.064	285	0.079
	4 – 5 cm	0.012	**0.004**	0.001	0.106	274	0.123
6	0 – 1 cm	0.016	**0.057**	0.006	0.142	194	0.220
	1 – 2 cm	0.013	**0.016**	0.002	0.072	150	0.103
	2 – 3 cm	0.014	**0.014**	0.002	0.146	224	0.177
	3 – 4 cm	0.006	**0.020**	0.003	0.074	398	0.103
	4 – 5 cm	0.006	**0.018**	0.001	0.088	360	0.114
9	0 – 1 cm	0.018	**0.091**	0.006	0.806	340	0.920
	1 – 2 cm	0.011	**0.026**	0.005	0.387	240	0.430
	2 – 3 cm	0.015	**0.029**	0.004	0.342	252	0.390
	3 – 4 cm	0.011	**0.043**	0.004	0.215	308	0.273
	4 – 5 cm	0.007	**0.038**	0.003	0.100	370	0.148
Row	**Depth**	Na^+	NH_4^+	K^+	Mg^{2+}	Ca^{2+}	**Sum cations**
3	0 – 1 cm	0.048	0.004	0.075	0.007	0.082	0.216
6	0 – 1 cm	0.130	0.005	0.163	0.003	0.054	0.355
9	0 – 1 cm	0.253	0.004	0.190	0.005	0.161	0.613

The different ion concentrations were expressed in mass-% of the sample. To estimate the molar concentration in mol/l and calculate the according activity the following steps are necessary:

$$c_i = \frac{m_i}{m_{total}} = m_i \frac{1}{m_{brick} + \sum_i m_i} = \frac{m_i}{m_{brick}} \left(\frac{1}{1 + \frac{\sum_i m_i}{m_{brick}}} \right) = \frac{m_i}{m_{brick}} b \quad (4)$$

with:

c_i – concentration of ion i in mass-%

m_x – mass of ion i, brick or total content

$\frac{\sum_i m_i}{m_{brick}} = \frac{\sum_i m_i}{m_{total} - \sum_i m_i}$ this and the constant b can be calculated with Table 1

In case the cations weren't analysed (depths > 1 cm, see Table 1), the average fraction of anions (43.3 %) was used to estimate the total sum of ions.

Formula (4) could be transformed in:

$$m_i = \frac{c_i m_{brick}}{b} = \frac{c_i}{b} \rho_{brick} V_{brick} \quad (5)$$

with ρ_{brick} = 1790 kg/m^3 (bulk density), V_{brick} set to 1 l, the maximum water available porosity = 23.2 % and under the assumption that all pore space is filled, the molar concentration can be calculated by:

$$c_i^{mol} = \frac{m_i}{m_i^a \; porosity_{brick}} \text{ in [mol/l]} \quad (6)$$

with: m_i^a – atomic mass of ion i, e.g. for Cl^- = 35,45 g [11]

The activity can be calculated with the mean activity coefficients $\gamma_\pm$ according to the formula given in (1). Mean activity coefficients for sodium chloride were taken from [7]. To estimate the values in between a fit function was calculated for the concentration range 0.005 and 0.2 mol/l.

$$y = A_1 e^{-\frac{x}{t_1}} + A_2 e^{-\frac{x}{t_2}} + y_0 \quad (7)$$

with: A_1 = 0.1845, t_1 = 0.1138; A_2 = 0.0735, t_2 = 0.0123, y_0 = 0.7022. The coefficient of determination was R^2 = 0.99979.

3 RESULTS

3.1. Potential difference in May 2011

First results [2] showed strong oscillations of potential difference even in sunny periods without rain (example May 2011, see Figure 3). This behaviour arises especially at ISEs in lower rows (3 and 6) and nearer to the surface (depth 2 cm and 6 cm). The amplitudes up to 200 mV are too high and cannot be explained with temperature differences between ISE and reference electrode in the Nernst limit (1). On the other hand ISEs at the rising solution limit near to the surface (row 9 and 12 at depth 2 cm) showed clearly Nernst behaviour [3]. The potential difference in row 3 behaves like the temperature difference between a sensor near the reference electrode and a surface near sensor. This difference is due to the sun insolation on the south side of the wall (front side). The potential difference is well above the solution value, which is reached only by minima in 2 cm and 6 cm depth. The solution value is fully crossed only by the ISE in row 12 depth 2 cm, which shows as well low oscillations.

A calculation based on mean values for potential difference and temperature (row 9 depth 2 cm: E = 163.8 mV, T = 28.6 °C) results in an activity of a_{Cl^-} = 0.0039 mol/l according to formula (3) [3]. By using this activity and the actual temperatures the curve of the ISE at row 9 depth 2 cm could be reproduced with (1) (Figure 3). The potential difference of the ISE in row 12 is decreasing, which corresponds to a higher concentration of Chloride in the pore solution around this ISE. The curve could be calculated by using (1) and an increasing activity from 0.5 to 1.4 of the solution activity between 27th and 31st May 2011 (Figure 3).

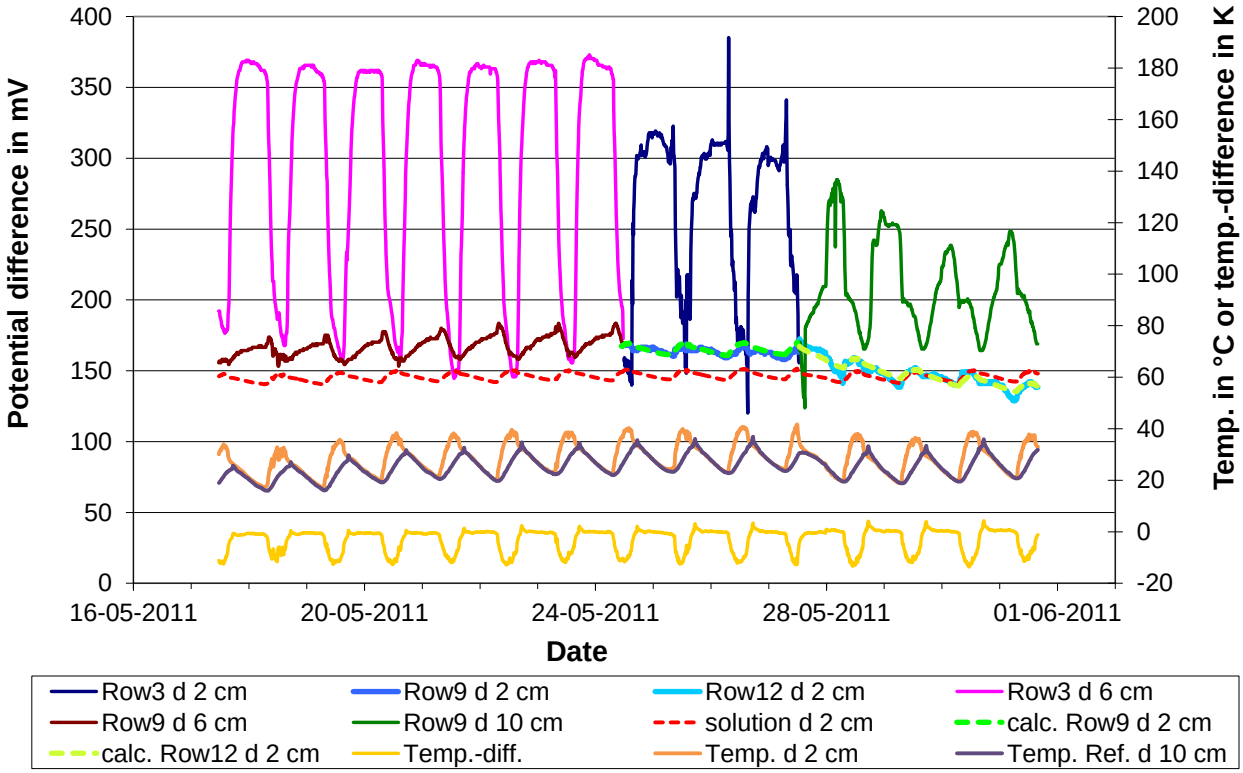

Figure 3. Potential difference of several ISEs in a sunny period in May 2011. The lower parts shows temperatures in different depths and the temperature difference between a sensor near the reference electrode (rear side, depth 10 cm) and a sensor near the surface (depth 2 cm). Calculated potential differences for the brine solution (c = 0.05 mass-% NaCl, a_{Cl^-} = 0.0078) and the ISEs in row 9 (a_{Cl^-} = 0.0039) and 12 (activity between 0.5 and 1.4 of solution value) are given.

3.2. Comparison with salt analysis

To check whether this reflects real concentrations a comparison was done with drill dust samples taken end of March 2011 at the end of a 4 month drying period without capillary suction during winter. Due to the strong daily variations average values of potential difference of multiples of full days (24 h) were taken. Only sunny periods were used, because rain on the wall results in large drops of potential difference. The comparison indicated qualitative comparable behaviour of potential difference in May 2011 and salt analysis by ion chromatography on dust samples from end of March 2011 [2, 3].

By using average values for potential difference and temperature, chloride activities were calculated for the ISE measurements according to (3). The salt analysis data are given in mass-%. Chloride activities were calculated according to the procedure described in Chapter 2.3. The results are displayed in Figure 4 in vertical and depth profiles.

The chloride activities from the dust samples are well above the brine solution activity, except for two samples from row 3. The ISE Chloride activities show qualitatively the same behaviour for the depths 2 and 6 cm as the drill dust samples but the estimated activity is around 1 to 2 orders of magnitude lower. Even the highest activity at row 12 and depth 2 cm didn't reach the brine solution value. The latter one is caused by averaging a decreasing potential difference. The real data show an intercept with the brine solution curve to the end of the period (Figure 3).

The drill dust samples were taken at the end of a 4 month drying period with no capillary suction at the wall base. After the drilling the dust was dried, therefore they contain the total amount of salts crystallized and dissolved. The highest level at row 9, depth 0 to 1 cm corresponds to an amount of 2.6 kg/m3 sodium chloride. The method didn't allow discriminating between dissolved and crystalized

part, but the ISEs react only on the dissolved part. The numerical simulation [4] predicts for the same zone and time about 2.0 kg/m^3 of crystallized and 0.8 kg/m^3 of dissolved sodium chloride. Therefore the total amount of sodium chloride is a factor of 3.5 higher than the dissolved part.

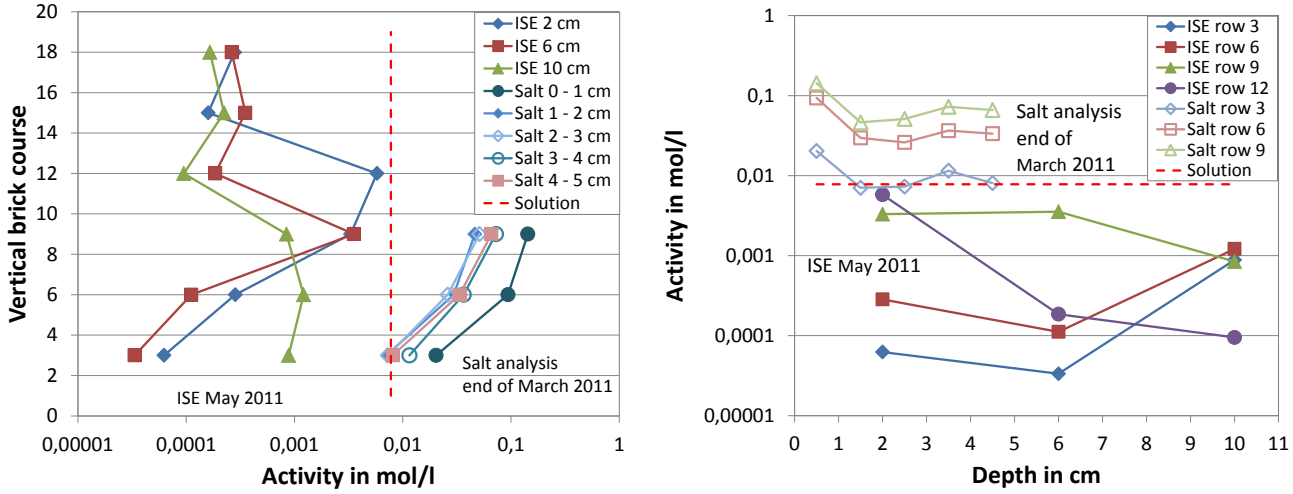

Figure 4. Quantitative comparison of salt analysis from end of March and ISE measurements in May 2011. Left: Vertical profile. Right: Depth profile.

3.3. Start of capillary suction

Figure 5 shows the results of the numerical simulation with an extended model to cover as well non-isothermal conditions [5]. The simulation uses daily averages of temperature and relative humidity from a climate station nearby. The time period used is 1st July 2010 to 30th August 2010 and the capillary suction started at the first day. This is slightly different from the real test wall conditions, were the capillary suction started at 21st of July. The difference in climate conditions should be not too large, if only daily variations were considered. Figure 5 includes maps for dissolved salt concentration and crystallised salt (both sodium chloride). The maps cover 15, 30, 45 and 60 days after the start of capillary suction. The ISEs react on dissolved chloride. Figure 6 shows maps of average values of potential difference before and after 2, 9, 19 and 64 days of capillary suction. The spatial extension of these maps corresponds to the rectangular area shown in Figure 5 at map (a, left). Dissolved salt concentration [5] and potential difference agree qualitative for the most evolved periods after 60 days in Figure 5 (map (d, left)) and after 64 days in Figure 6, considering the low spatial resolution of the ISE network.

The real time potential difference data of the period in September 2010 are given in Figure 7 for a depth of 2 cm. As in May 2011 the potential difference in row 3 and 6 show strong daily variations. The curve at row 9, depth 2 cm increases with only small variations. An increase in potential difference corresponds to a decrease of activity (Figure 2). This is an indication that the concentrated pore solution rises and the position of the maximum concentration is above the ISE in row 9. From 22nd to 24th September the curve can be reproduced by the use of (1). The applied factors of the solution activity are 1.9, 1.1 and 0.7 during the nights with nearly no temperature difference and a linear interpolation between these values during the days. The calculated curve is comparable with small differences during the day.

The data of the ISEs in depth 10 cm show less daily variations (Figure 8). The ISEs in row 6 and 9 are influenced from the temperature difference, whereas the ISE in row 3 show only smooth variations. The extrema follow the temperature curve, but the potential difference variation is higher than expected if only temperature variations are considered (see insert in Figure 8). If considered as Nernstian behaviour the variation can be explained by a daily variation of the pore solution concentration between 0.35 and 0.2 of the brine solution activity according to (1). The lower activity

appears at early evenings (around 6 pm) and the higher activity at late mornings (around 10 am). For the ISEs in row 6 and 9 an effect of the temperature difference between reference sensor and sensor in 2 cm depth is visible, but the sign is reversed for row 9 (Figure 8). At surface near electrodes (row 3 and 6) the evaporation leads to a sharp drop of potential difference at around 8 am and a less sharp increase at around 6 pm (Figure 7). It is not as smooth as the process in 10 cm depth at row 3.

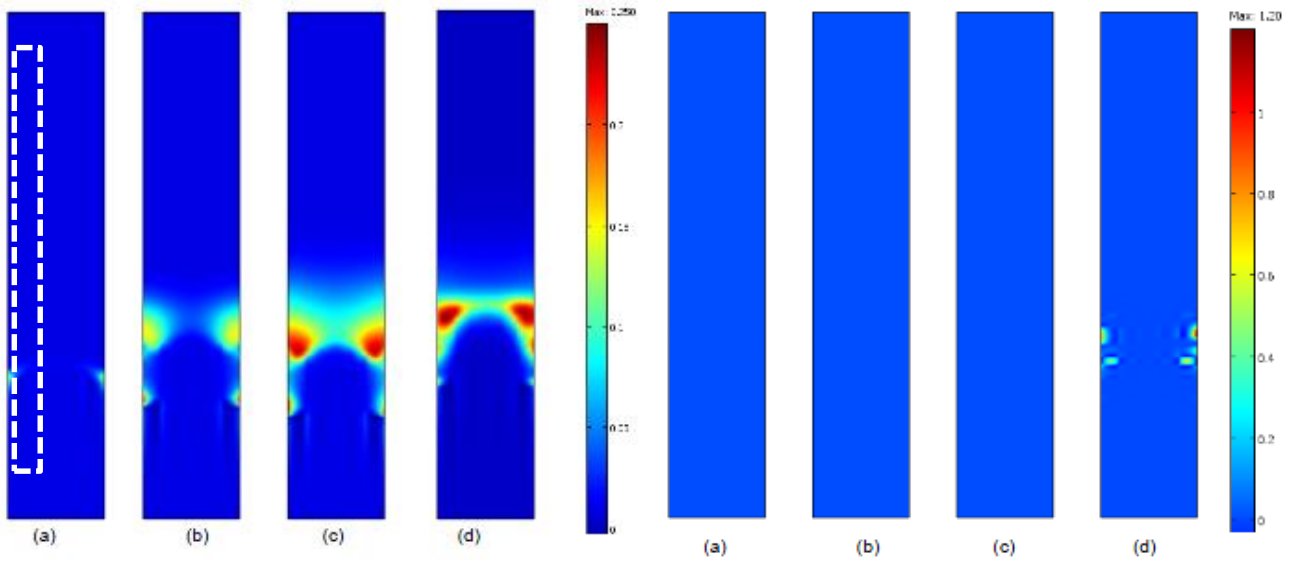

Figure 5. Maps of dissolved salt concentration (left) and crystallised salt (right) after 15, 30, 45 and 60 days. The rectangle in map (a, left) defines the area of installed ISEs at rows 3, 6, 9, 12, 15 and 18 at depths 2, 6 and 10 cm. Source: [5].

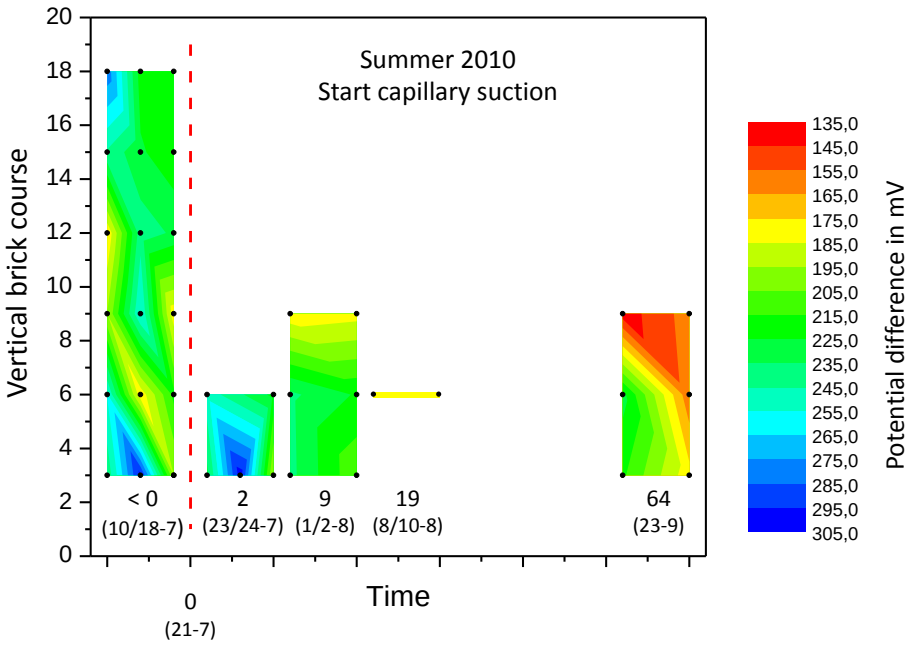

Figure 6. Maps of average values of potential difference before and after 2, 9, 19 and 64 days of capillary suction (start 21st July 2010, red line). The black dots define the involved measuring ISEs at different depths and periods. The time averages used to generate the maps are given in brackets.

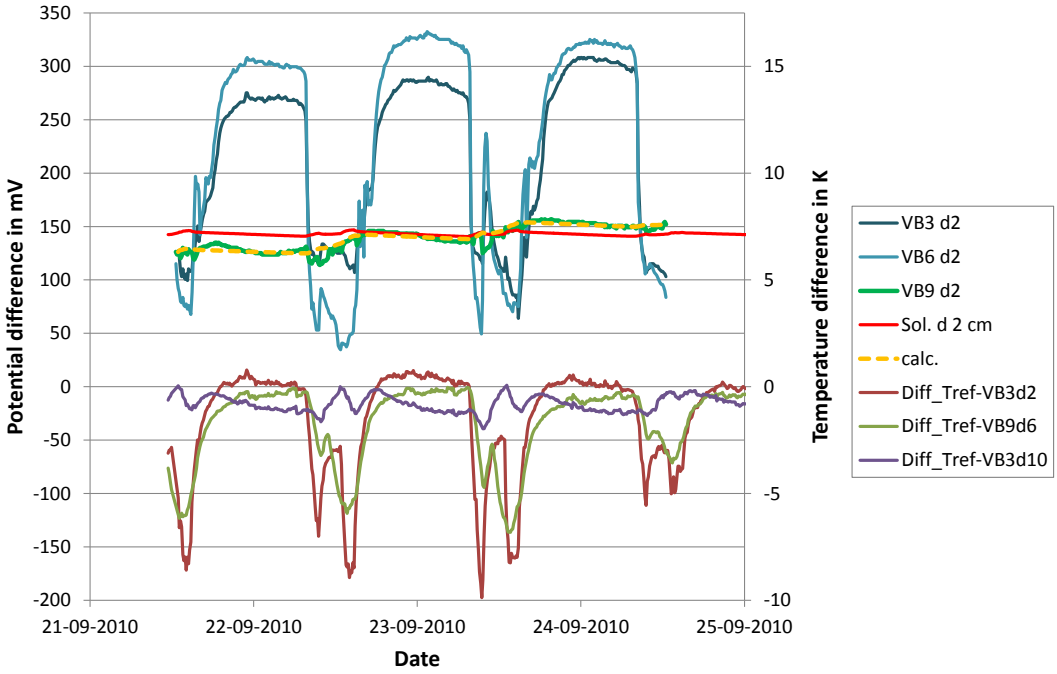

Figure 7. Surface near measurements (depth 2 cm) at sunny days in September 2010. Upper part: Potential difference for rows 3, 6 and 9. Lower part: Temperature difference between the temperature sensor near to the reference electrode, depth 10 cm at the rear side, and the sensors at the front side in 2, 6 and 10 cm depth. The expected potential difference for the brine solution (a_{Cl}- = 0.0078) is displayed as red line. The dashed orange line is calculated by (1) with the solution activity multiplied by the factors 1.9 (22-09), 1.1 (23-09) and 0.7 (24-09) during the nights and linear interpolations in between during the days.

By remapping the potential difference and temperature data on a common time scale (10 minutes intervals) the correlation between these data can be analysed. Figure 9 shows the correlation between potential difference of surface near ISEs (depth 2 cm) in row 3, 6 and 9 with temperature difference between reference sensor and surface near sensor in 2 cm depth. The ISEs in row 3 and 6 show a strong correlation for temperature differences in the range 1 to -2 K and below only lower variations, like the ISE in row 9 for the whole range. It seems that the sun insolation drives a bipolar behaviour of the potential difference at row 3 and 6. As soon as the sun arrives the potential difference drops and arrives in the first state. If shadow occurs for a certain time, it rises and drops again (Figure 7), and when the sun sets it rises and reaches the second state. The shadowing might be due to another wall in front of the test wall and the lower sun height in September compared to May, because in May are no variations during daylight in potential difference and temperature difference visible (Figure 3).

4 DISCUSSION

In the period of May 2011 the wall was the second time supposed to a capillary suction of around 50 to 60 days. The strong oscillations of the potential difference in row 9 at depth 10 cm indicate that the brine solution has arrived at this height in the central part of the wall (Figure 3). The moisture condition is different to the relative dry period at end of March, where the dust samples were taken. Part of the salts could be dissolved and redistributed within the wall. The numerical simulation [4] shows only data for 8 month (corresponding to end of March) and 12 months. May 2011 would be in between at month 10. The supersaturation ratio and the amount of crystallised salt are given. Partly crystallised salt appear at 8 and 12 months and the supersaturation ratio reaches 1 a little above the solution front near to the surface after 12 months.

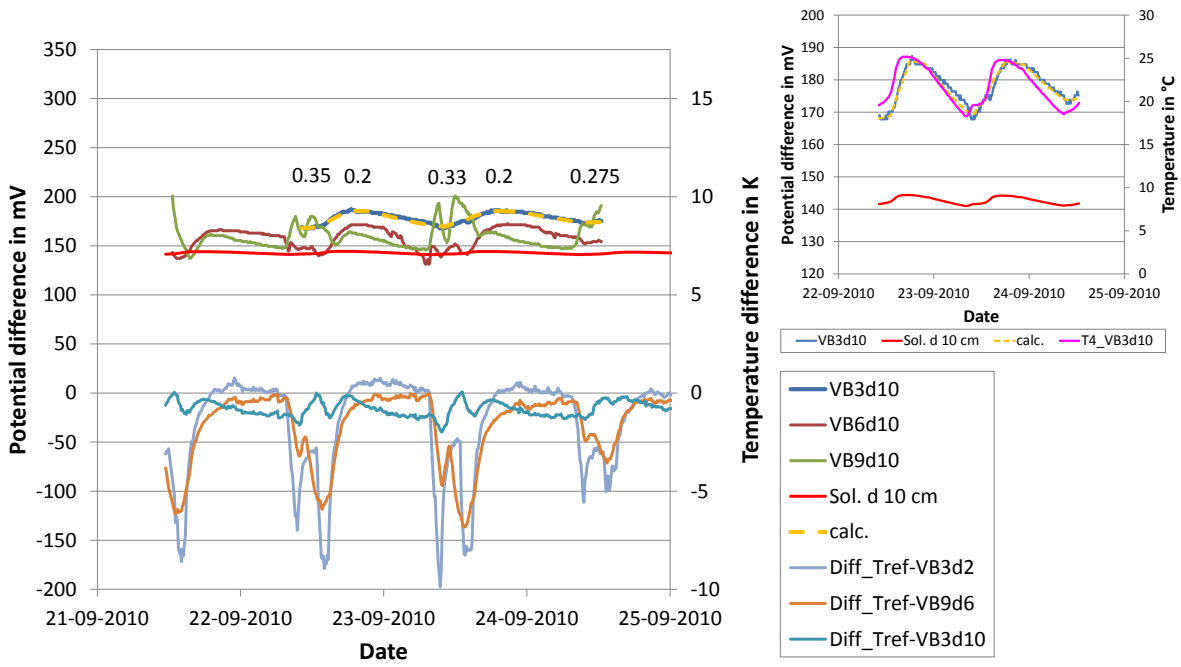

Figure 8. Measurements in 10 cm depth at sunny days in September 2010. Upper part: Potential difference for rows 3, 6 and 9. Lower part: Temperature difference between the temperature sensor near to the reference electrode, depth 10 cm at the rear side, and the sensors at the front side in 2, 6 and 10 cm depth. The expected potential difference for the brine solution (a_{Cl}- = 0.0078) is displayed as solid red line. The dashed orange line is calculated by (1) with the solution activity multiplied by the factors given above the curve for row 3. The insert on the right shows an overlay of the potential difference and temperature curves for row 3 depth 10 cm.

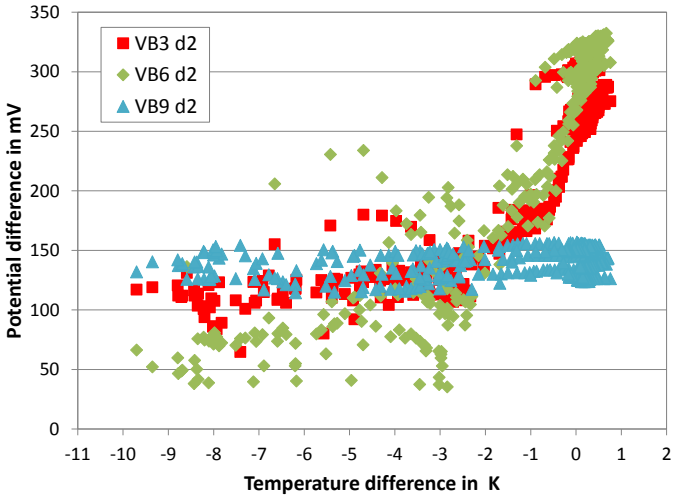

Figure 9. Left: Correlation between potential difference of surface near ISEs (2 cm depth) in row 3, 6 and 9 with temperature difference between the reference sensor and the sensor in 2 cm depth.

Crystallisation needs a saturated solution. The solubility of sodium chloride is 359 g/l [12]. The molar concentration is 6.14 mol/l and the activity around 5.37 mol/l ($\gamma_{\pm}$ = 0,874 for 5 mol/kg [7]). The Nernst potential for such a solution would be around -25 mV according to (1). Even in the vicinity of crystallised salt the pore solution should be highly concentrated, certainly higher than the brine

solution at the base. If the surface near ISEs in row 9 and 12, which show Nernst behaviour, are near to the maximum salt concentration in non-saturated pore space, the measured potential difference didn't reflect this. The measured potential is near to the activity of the brine solution (maximum factor is 1.4) and didn't show high concentrations near saturation. Therefore additional effects must be considered. In [3, 9, 13, 14] the influence of diffusion potentials and other disturbing factors are discussed.

The principle measurement setup is shown in Figure 10 (Middle). Due to the position of the electrodes there could be an influence of the porous medium in between. At least two alkaline mortar layers are between the reference electrode and an ISE even for the lowest course. Concentration differences in the pore solution are expected for higher rows. Additional the daily insolation on the front side drives evaporation which could lead to advection of dissolved ions in direction to the surface. Therefore non-varying and varying influences are expected and the measured potential difference is a time dependent sum of different effects (see Figure 10, right). The situation for the period in September 2010 is similar. The only difference is that the measured potential differences reach lower values as in May 2011. This might be due to the first capillary suction period. There are no salts in the pore space which hinder the uptake of solution as for May 2011.

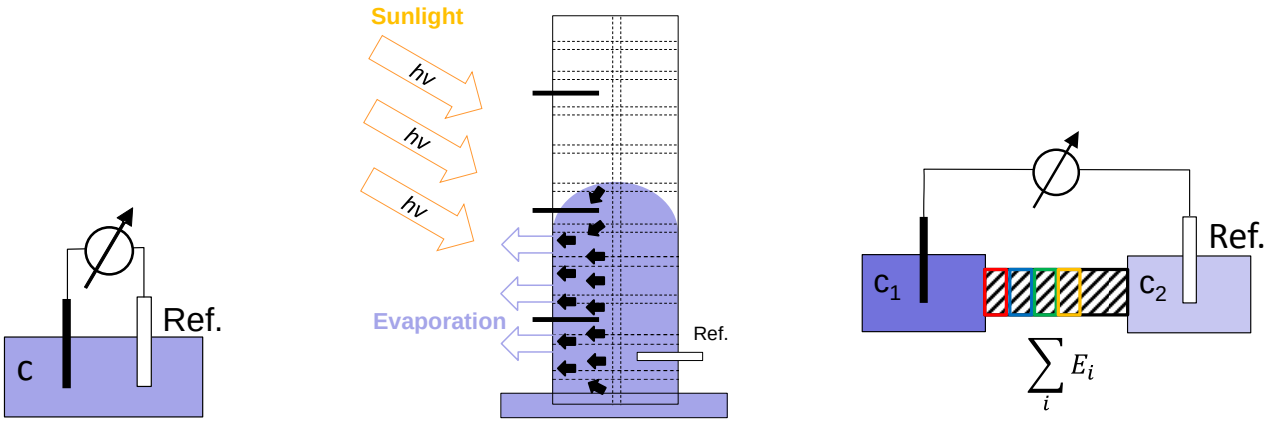

Figure 10. Left: Ideal measurement principle in the same solution. Middle: Model of the test wall with capillary suction and evaporation driven advection of ions during the day. Right: Real measurement principle with the influence of diffusion potentials and other disturbing factors.

5 CONCLUSIONS

The measured potential difference at the test wall is influenced by several effects. The comparison with salt analysis on drill dust samples and with numerical models indicates that the estimated activity didn't reflect the real chloride concentration. Some of the measured curves near to the surface to the main crystallisation level show Nernst behaviour according to (1). Therefore the additional potential differences must be of constant or low varying type. This could be differences in the porous media, including perm-selectivity, chemical influences (e.g. alkalinity) and concentration differences, which are of interest. With further research on defined samples and conditions this will be estimated.

Strong daily oscillations of the measured potential give an insight in ongoing transport processes. They occur in solution saturated regions mainly near to the surface. A numerical model, which include ionic transport for diffusion, migration and advection was used in [14] to model the transport of different ions in a concrete samples with three layers of different chloride content. A combination of the hygrothermal model [4, 5] with this model could be a possibility to model the observed transport processes.

In principle potential difference measurements are valuable to provide a qualitative understanding of salt movements in real buildings. If further electrodes for other relevant ions (e.g. sulphate, nitrate,

etc.) are available and the occurring effects of disturbing potentials are solved, a quantitative understanding will be possible. Tests within the SMooHS project showed results with less variations if the ISEs are installed at an inner face of a façade wall (e.g. at the chapel of Schönbrunn palace) [15].

ACKNOWLEDGEMENTS

The project "Smart monitoring of historic structures – SMooHS" was funded by the European Commission within the 7th framework programme under Grant Agreement Number 212939 and partly for the German partners by the Research Initiative "Zukunft Bau" of BBSR (Bundesinstitut für Bau-, Stadt- und Raumforschung) under Reference Number SF – 10.08.18.7- 08.35/ II 2 – F20—08-37. The authors are responsible for the content. We acknowledge the facilities of the LISG Lab of DICAM Dept., Bologna University. We thank Christiane Bock-Carstens for performing the calibration measurements of potential electrodes and Corinna Luz for the salt analyses by ion-chromatography.

REFERENCES

[1] www.smoohs.eu *Smart Monitoring of Historic Structures - SMooHS*, Project reports, EU-FP7 Project, Ref. no.: 212939, Duration: 01-12-2008 to 30-11-2011, 2011.

[2] Colla, C.; Gabrielli, E.; Grüner, F.; Frick, J.: Monitoring of Salt Content and Mobility in Masonry Materials. In: *Cultural Heritage Preservation*, *Proc. of the 1st European Workshop on Cultural Heritage Preservation EWCHP-2011*, Berlin, Germany 26th – 28th September 2011, ed. M. Krüger, Fraunhofer IRB Verlag, ISBN 978-3-8167-8560-6, 2011.

[3] Frick, J.; Colla, C.; Gabrielli, E.; Grüner, F.: Seasonal Monitoring of Salt Movenment in Masonry Materials. In: *Proceedings of the 2nd European Workshop on Cultural Heritage Preservation EWCHP-2012*, Kjeller, Norway 23rd to 26th September 2012.

[4] Castellazzi, G.; Colla, C.; de Miranda, S.; Formica, G.; Gabrielli, E.; Molari, L.; Ubertini, F.: A coupled multiphase model for hygrothermal analysis of masonry structures and prediction of stress induced by salt crystallization. *Construction and Building Materials*, 41 (2013), 717-731.

[5] Castellazzi, G.; de Miranda, S.; Grementieri; L.; Molari, L.; Ubertini, F.: Assessment of Salt Crystallization through Numerical Modelling. *Cultural Heritage Preservation, Proc. of the 3rd European Workshop on Cultural Heritage Preservation EWCHP-2011, Bozen/Bolzano, Italy, 16th – 18th September 2013, eds. A. Troi & E. Lucchi,* European Academy of Bozen/Bolzano (EURAC), ISBN 978-88-88307-26-8, 2013.

[6] Angst, U.; Elsener, B.; Larsen, C.K.; Vennesland, Ø.: Potentiometric determination of the chloride ion activity in cement based materials. *J. Appl. Electrochem*., 40 (2010) 3, 561-573.

[7] *Handbook of chemistry and physics*, 91st edn., CRC Press: Boca Raton, online and printed version 2010–2011.

[8] Shreir, L.L.; Jarman, R.A.; Burstein, G.T.: *Corrosion*, vol 2, 3rd edn. Butterworth Heinemann: Oxford 1994.

[9] Atkins, C.P.; Carter, M.A.; Scantlebury, J.D.: Sources of error in using silver/silver chloride electrodes to monitor chloride activity in concrete. *Cem. Concr. Res*., 31 (2011) 1207-1211.

[10] SI-Analytics GmbH personal communication.

[11] Wieser, M.E.; Coplen, T.B.: Atomic weights of the elements 2009 (IUPAC Technical Report), *Pure Appl. Chem.*, 83 (2011) 2, 359–396.

[12] http://en.wikipedia.org/wiki/Sodium_chloride *Sodium chloride***,** Wikipedia, accessed February 2014.

[13] Angst, U.; Vennesland, Ø.; Myrdal, R.: Diffusion potentials as source of error in electrochemical measurements in concrete, *Materials and Structures*, 42 (2009) 365–375.

[14] Angst, U.; Elsener, B.; Myrdal, R.; Vennesland, Ø.: Diffusion potentials in porous mortar in a moisture state below saturation, *Electrochimica Acta,* 55 (2010) 8545–8555.

[15] Frick, J.; Lehmann, F.; Menzel, K.; Pakdel, H.; Krüger, M.: Monitoring of salt content in mineral materials using wireless sensor networks, *Nondestructive Testing of Materials and Structures*, Proc. NDTMS-2011, May 15-18, 2011, Istanbul, Turkey, eds. O. Buyukozturk, M.A. Tasdemir, O. Gunes, & Y. Akkaya, RILEM Bookseries 6 (2012) 1103-1109.